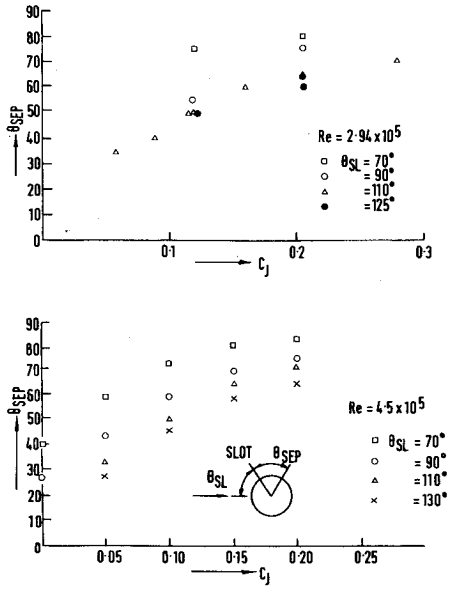

Fig. 1 Upper separation point, lifting cylinder.

defining Reynolds number as

$$R_e = [(P-p_{SL})bd/\rho v^2]^{1/2}$$

At large Reynolds number, the jet flow tends to become independent of viscosity[4]

$$\frac{(p_{SL}-p_S)}{(P-p_{SL})}\frac{d}{b} = f\left[\frac{\theta}{\theta_{SL}}, C_J{}^{1/2}\right]$$

Similar results can be stated for the angular position of separation θ_{sep} as

$$\theta_{sep} = f\left[\frac{b}{d}, \left\{\frac{(P-p_{SL})bd}{\rho v^2}\right\}^{1/2}, \frac{\theta_{sep}}{\theta_{SL}}, C_J{}^{1/2}\right]$$

If the position of separation is sufficiently far from the slot

$$\theta_{sep} = f\left[\frac{\theta_{sep}}{\theta_{SL}}, \left\{\frac{(P-p_{SL})bd}{\rho v^2}\right\}^{1/2}, C_J{}^{1/2}\right]$$

At large values of Reynolds numbers

$$\theta_{sep} = f[\theta_{sep}/\theta_{SL}, C_J{}^{1/2}] \quad (1)$$

Experimental Results and Conclusions

Figure 1 shows the two sets of separation point values taken from the pressure distribution measured by Herrick (1972) on a lifting cylinder of diameter 15.05 cm, with a slot of 0.6 mm wide at Reynolds number of 2.94×10^5 and 4.5×10^5. Pressure distributions were measured for various values of the jet momentum coefficient and slot positions. All the separation point data of Fig. 1 have been plotted in Fig. 2 in the co-ordinates of Eq. (1).

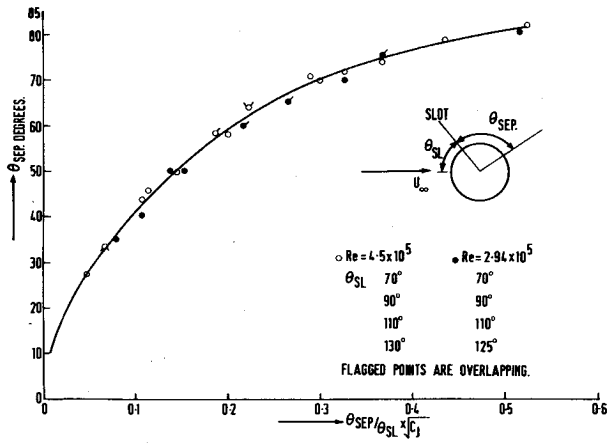

Fig. 2 Separation point correlation, lifting cylinder.

A clear agreement of a simple form of Eq. (1) can be seen in Fig. 2 establishing a good similarity. The angle between the separation point and the slot is therefore independent of Reynolds number (at sufficiently high Reynolds number) and is a function of the position of the slot and the jet momentum coefficient only.

References

[1] Cheeseman, I. C., "The Application of Circulation Control by Blowing to Helicopter Rotors," *Journal of the Royal Aeronautical Society*, Vol. 71, No. 679, July 1967, pp. 451–467.

[2] Cheeseman, I. C., "Circulation Controlled Rotor Aircraft," *Aircraft Engineering*, Vol. XLI, July 1969, pp. 10–16.

[3] Newman, B. G., "The Deflection of Plane Jets by Adjacent Boundaries—Coanda Effect," *Boundary Layer and Flow Control*, edited by G. V. Lachmann, Vol. 1, Pergamon Press, New York, 1961.

[4] Townsend, A. A., *The Structure of Turbulent Shear Flow*, Cambridge University Press, Cambridge, England, 1956.

[5] Herrick, G. E., "Wind Tunnel Tests on Circulation Controlled Circular Cylinders in Steady and Heaving Motion," Ph.D. thesis, Dept. of Aeronautics and Astronautics, University of Southampton, Southampton, England, 1972.

Miniature Probe for Transonic Flow Direction Measurements

F. W. Spaid,* F. X. Hurley,† and T. H. Hellman‡
McDonnell Douglas Corporation, St. Louis, Mo.

Probe Description and Calibration

Figure 1 includes a photograph and a sketch of the tip geometry of a probe developed to measure flow direction and stagnation pressure in the boundary layer and near wake of a transonic airfoil. The probe may be viewed as a smaller, flattened version of the multiple-tube configurations described in Refs. 1 and 2, and is intended for flow direction measurements in one plane. The advantages of this design are ruggedness, ease of fabrication, ability to measure flow direction at a point, and insensitivity to out-of-plane velocity components. The tip was fabricated from three pieces of 0.010 in. (0.25 mm) o.d., 0.005 in. (0.13 mm) i.d. stainless steel tubing which were squeezed around a 0.001 in. (0.025 mm) pointed shim, thus reducing the height dimension to 0.006 in. (0.15 mm). An Arkansas stone was then used to bevel both upper and lower surfaces to produce a tip height of approximately 0.0035 in. (0.089 mm). The desired face angles were fashioned by stoning in a jig. The space curves required for the three tubes to converge at the tip were formed manually by trial and error. Larger tubing and epoxy (cured at 250°F or 395°K) were used for bracing and for structural carry-through. A microscope and an optical comparator were employed during fabrication. The small tubes were frequently flushed with distilled

Received August 8, 1974. This research was conducted under the McDonnell Douglas Independent Research and Development Program in cooperation with the NASA Ames Research Center.

Index categories: Aircraft Testing (Including Component Wind Tunnel Testing); Subsonic and Transonic Flow; Research Facilities and Instrumentation.

* Scientist, McDonnell Douglas Research Laboratories. Associate Fellow, AIAA.

† Scientist, McDonnell Douglas Research Laboratories. Member AIAA.

‡ Lead Technician, McDonnell Aircraft Company.

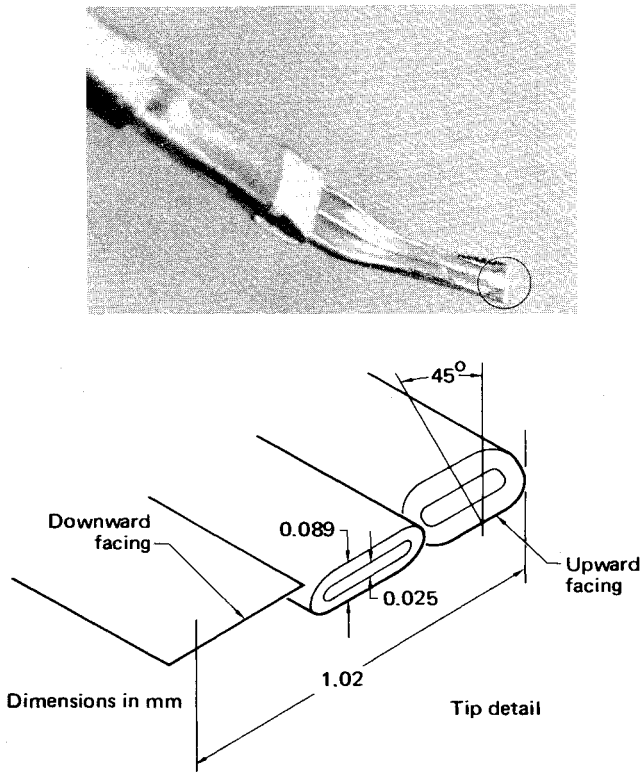

Fig. 1 Probe tip geometry.

water using a hypodermic needle; however, during the wind tunnel tests, back-suction with a volatile solvent proved more successful in keeping the tubes open.

The probe was calibrated with the aid of a small free-jet facility which was manufactured commercially for the calibration of hot-wire anemometers. The tip was placed in the inviscid core of the jet, which exhausted to atmosphere, and angles between the probe shaft and a reference plane aligned with the jet nozzle axis were measured to the nearest 0.1°. Figure 2 is a typical probe calibration curve presenting the flow inclination angle vs the difference between the pressures measured by the two outer tubes, normalized by the center tube pressure, for various Mach numbers. These results show that this method of data presentation is insensitive to Mach number for $M \geq 0.8$, and that the sensitivity of this technique for determining flow angularity decreases with decreasing Mach number.

The static pressure and stagnation temperature of the jet were essentially constant during the calibration of the probe, so that the Mach and Reynolds numbers near the probe tip were varied simultaneously. Although the body of data obtained from calibrations of other types of flow-angularity probes suggests that the variation shown in Fig. 2 is primarily a Mach number effect,[1] the present calibration data do not eliminate the possibility of an independent influence of Reynolds number. An investigation of the influence of Reynolds number on the probe calibration has not yet been conducted, because the static pressure and stagnation temperature of the tests in which this probe has been used were essentially the same as those of the calibration. Consequently, the variation of Reynolds number with Mach number in both cases was nearly the same.

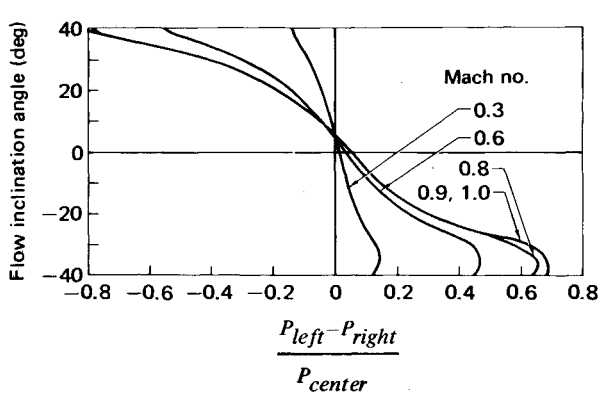

Fig. 2 Probe calibration curves.

The influence of proximity to a surface on the indicated flow inclination angle was investigated by a series of calibration runs in which a razor blade was mounted in the jet and aligned with the flow. The error remained small, less than $\pm 0.5°$, when the distance from the wall was greater than 0.025 in. (0.63 mm). Other potential sources of error in the measured flow inclination angle, such as shear and turbulent fluctuations, have not yet been investigated.

Example of Data

A sample of data obtained with the probe is given in Fig. 3. These measurements were obtained in the near wake of a supercritical transonic airfoil.[3] The 6-in. chord model spanned the test section of the Two-by-Two-Ft Transonic Wind Tunnel at NASA Ames Research Center. The combination of test-section pressure levels and small probe tip dimensions caused significant time delays for stabilizing the indicated pressure. Approximately 5 sec were required to obtain an accurate reading at the lowest pitot pressure. These data were taken at center span, 5% chord downstream of the trailing edge. The z/c axis is normal to the freestream flow direction, with the origin at the upper corner of the trailing edge. At this combination of Mach number and lift coefficient, the airfoil drag coefficient is substantially higher than its low-speed value, and the upper-surface boundary layer is separated at the trailing edge.

Figure 3a is a speed profile obtained from center-tube measurements. Speeds were computed by conventional methods, using freestream values of stagnation temperature and static pressure. The trailing-edge pressure coefficient was 0.055 in this case, so that the use of freestream static pressure in the data reduction should lead to only small errors in the computed speeds and negligible errors in flow inclination angles. The corresponding flow inclination profile is shown in Fig. 3b, where upwash is considered positive. The scatter is representative of the precision in flow angle measurement which was achieved during this series of experiments. The data are plotted in vector form in

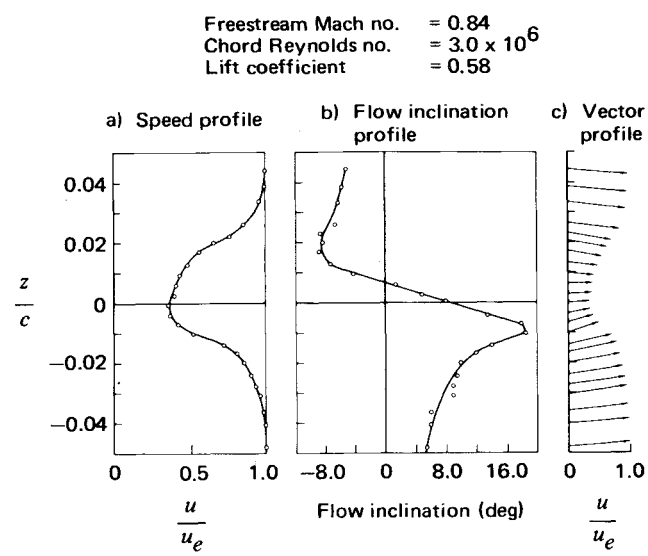

Fig. 3 Near wake survey data from test of supercritical airfoil.

Fig. 3c. The position of the tail of each arrow on the ordinate corresponds to the measurement location. The arrow is drawn in the indicated flow direction, with a length proportional to the speed. This figure is representative of the type of detailed flowfield information that the probe was designed to provide. The maximum gradient in flow angularity, i.e., the maximum convergence of streamlines, is seen to occur where the speed is the lowest. This is the case in the vicinity of a free stagnation (wake closure) point, which must exist slightly upstream, nearer the finite thickness (1% chord) trailing edge.

Conclusions

A probe for the measurement of flow direction in one plane, as well as of stagnation pressure, has been constructed, calibrated, and used in a study of flow about a transonic airfoil. The tip dimensions are comparable to those of the smallest boundary-layer pitot probes in current use, while the resulting data contain an extra dimension of information.

References

[1] Bryer, D. W. and Pankhurst, R. C., *Pressure-Probe Methods for Determining Wind Speed and Flow Direction*, Her Majesty's Stationery Office, London, 1971.

[2] Dudzinski, T. J. and Krause, L. N., "Flow-Direction Measurement with Fixed-Position Probes," TM-X-1904, Oct. 1969, NASA.

[3] Hurley, F. X., Spaid, F. W., Roos, F. W., Stivers, L. S., Jr., and Bandettini, A., "Supercritical Airfoil Flowfield Measurements," submitted for publication to the *Journal of Aircraft*.

Test Time Determination by End Wall Pressure Measurement in an Arc-Driven Shock Tube

A. J. MULAC* J. L. MARK,† AND J. A. GUZMAN‡
Sandia Laboratories, Albuquerque, N. Mex.

SUCCESSFUL shock tube experimentation depends critically on the separation of the shock front and contact surface. Separation is achieved readily in the classical diaphragm shock tube. However, in high-energy devices such as the Sandia arc-driven shock tube facility, separation may not always occur and is not readily predicted.

This Note presents shock-wave-contact surface separation measurements by means of a fast rise time, long-dwell, end-wall pressure gage. The end-wall pressure is a sensitive indicator of the interactions between the reflected shock wave and the contact surface, and provides a measure of the density profile behind the incident shock. The measurement of end-wall pressure has been developed into a very powerful shock tube diagnostic technique by Baganoff and Hanson.[1-4]

The application of the end-wall technique to test-time determination is based on the density or more specifically, acoustic impedance discontinuity at the contact surface. There are three possible interactions between the reflected shock and the contact surface. If the driver gas impedance is larger than the test gas impedance, a compression wave will reflect and produce a pressure rise on the shock tube end wall. If the driver gas impedance is less than the test gas impedance, a rarefaction wave will reflect and produce a pressure drop on the shock tube end wall. When the impedance is matched across the contact surface, the reflected shock will be transmitted and no signal will be received on the end wall.

The end-wall pressure gage used in this study is of the type described by Hanson and Baganoff.[5] The gage is a 10.16 cm diam pressure bar with a dual capacitive element in the center to detect normal stress. The gages used in this study were calibrated with a separate pressure-driven shock tube. The calibration shots were chosen to provide a pressure step with no real gas effects. The calibrations confirmed the linearity of the end-wall gages and provided a gage factor for data reduction. Because of the severity of the arc-driven shots, the calibration of the pressure gages was checked after each shot. Gage lifetime ranged from 4–20 shots; a total of 9 gages were used in this study. The end-wall pressure gages were used in a differential mode. One capacitive element was charged to $+2$ kV and the other to -2 kV. Noise due to ionization in the test gas and precursors is independent of the charge polarity; however, the pressure signal is sensitive to charge polarity. Thus, the signals from the two elements were subtracted to eliminate the noise and double the gage sensitivity.

The Sandia arc-driven shock tube and its performance have been described previously.[6,7] For these experiments a 76-cm-long arc driver and a 12-cm-diam driven tube was used. The driven tube was evacuated to 10^{-2} torr or less before each shot. The combined leak/outgas rate was $\leqq 2\times10^{-3}$ torr/min. Since the dwell time of the end-wall pressure gage was limited to 25 μs, very low initial pressures were necessary to see the contact surface wave interaction on the end wall. P_1 values of 0.1 torr and 0.5 torr were used and measured with a capacitive manometer (Baratron gage). The uncertainty in the initial pressure was $\Delta P_1/P_1 \leqq 10\%$. This large uncertainty was due primarily to the leak/outgas rate and the time between filling and arc initiation.

The shock speed in these experiments was determined from time of arrival data at several shock detectors (impedance probes and piezoelectric pressure gages). Shock attenuation was negligibly small over the approximately 1 m measurement span. Shock speed uncertainty was $\Delta u/u \leqq 5\%$.

Figure 1 presents end-wall pressure histories for three shock speeds from 7.8 to 10.4 km/sec in 0.1 torr nitrogen. The monotonic pressure rises are terminated by slight decreases in pressure followed by strong rises and subsequent oscillations. The measurement time (gage dwell time) for each of these shots was 25 μs. The slight fall in pressures is interpreted as a reduced impedance mixing region in front of the contact surface which is indicated by the sharp pressure rise. The end of the test time

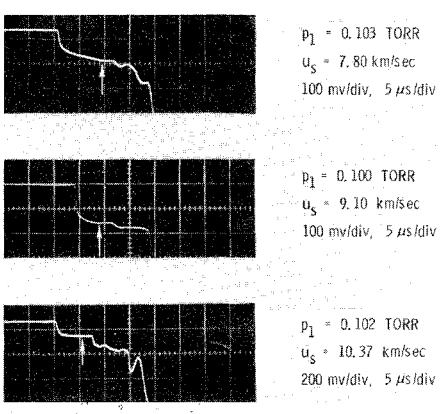

Fig. 1 End-wall pressure records for 0.1 torr nitrogen experiments. The departure of the trace represents shock front arrival at the end wall. The arrows indicate the arrival of the disturbance from the mixing region in front of the contact surface.

Received August 27, 1974. This work was supported by the United States Atomic Energy Commission.

Index category: Nonsteady Aerodynamics.

* Member of Technical Staff, Project Leader. Member AIAA.

† Member of Technical Staff; presently at Boeing Airplane Company, Seattle, Wash.

‡ Engineering and Science Assistant.